A Novel Periodic Energy Control for Non-isolated DC-DC Converters with Overshoot Suppression

Tianlu Ma, C. Q. Jiang, *Senior Member, IEEE*, Xiaosheng Wang, Jingchun Xiang, Liping Mo, and K. T. Chau, *Fellow, IEEE*

Abstract- **A novel periodic energy control (PEC) strategy for DC-DC converters is proposed in this letter, where the port nearest to the load is selected as the energy control target, considering the loss of switching and passive components. A simplified energy calculation method is derived to replace the integration methods in terms of the possible error during successive integral calculations, meanwhile reducing the computational burden. Furthermore, PEC is extended to other non-isolated DC-DC converters. Finally, the high accuracy of the simplified energy calculation is proven in simulations, and a 100-kHz synchronous buck converter is established to verify the proposed PEC. During the reference voltage stepping, the inductor saturation and overshoot occur in proportional-integral (PI) control by tuning the duty cycle, whereas the output voltage can track the reference within 1.4 ms without any overshoot in single-loop PEC, which illustrates its advantage in overshoot suppression. Also, dual-loop PEC shares the same conclusion.**

Index Terms— **DC-DC converters, overshoot, and periodic energy control (PEC).**

I. Introduction

Non-isolated DC-DC converters are popular circuits for power conversion and are widely applied in the power grid, laptops, solar photovoltaic systems, etc. In addition, non-isolated DC-DC converters are often cascaded with other power conversion equipment to regulate output due to their small size and cost savings. For instance, a buck and a boost converter are added before the inverter and after the rectifier of a wireless power transfer (WPT) system to track the maximum efficiency point [1].

The high performance of the converters relies on their control strategies, and the control methods should meet the requirements in different application scenarios, i.e., a fast dynamic response, stable output, or small overshoot. The proportional-integral-derivative (PID) control was applied to regulate the output voltage of the boost converter [2]. Also, a robust PID controller under a feedforward framework was proposed to achieve a fast closed-loop dynamic response with a boost converter, and the modified direct synthesis approach was proven better than internal model control in disturbance rejection [3].

An undershoot and overshoot in the output voltage might occur when the voltage or current reference changes, which can mitigate the sustainability and reliability of components and the whole system. An auxiliary circuit was employed to reduce the output voltage overshoot of a buck converter, and the control strategy was presented in terms of unloading transient [4]. Similarly, an auxiliary output stage was paralleled to the converter, and the PID control was conducted by a digital controller to make a trade-off between fast dynamic response and high efficiency, and the overshoot can be decreased by 50 % [5]. However, there is no doubt that the auxiliary circuits will cause additional loss. The traditional sawtooth wave generator was improved to optimize the capacitor characteristics during charging and discharging [6], and a lower overshoot and shorter recovery time were achieved. Meanwhile, the design of the sawtooth wave generator requires a complex circuit. Charge balance control [7], [8] and time-optimal control [9] are two methods to improve the system's dynamic response by optimizing the charging and discharging time of the output filter capacitor. The overshoot and recovery time can be reduced, but only one condition of the load current step was considered. In [10], a current-mode control method applied for boost converters was proposed to suppress overshoot, and a complicated dual-loop structure needs to design against the source voltage and load current disturbances. Model predictive control (MPC) [11], which can be divided into finite control set (FCS) MPC and continuous control set (CCS) MPC, has a fast dynamic response, and its basic principle is that the system trajectory in future moments can be predicted by a mathematical model. An FCS-MPC was applied to a noninverting buck-boost DC-DC converter in [12], and it has less overshoot compared with proportional-integral (PI) control. However, MPC relies on a high-accuracy mathematical model. Thus, the digital controller suffers a huge computational burden.

In this letter, a novel periodic energy control (PEC) for non-isolated DC-DC converters is proposed, which can suppress the overshoot effectively, thus, improving the system's sustainability and reliability. In order to reduce the computational burden and improve the robustness of PEC, a simplified energy calculation is proposed. Also, it is extended

Manuscript received April 14, 2023; revised May 15 and June 10, 2023; accepted June 22, 2023. This work was supported in part by a grant (52107011) from the Natural Science Foundation of China (NSFC), China; in part by a grant (ITS/068/21) from the Innovation and Technology Commission, Hong Kong SAR; in part by an ECS grant (21200622) from the Research Grants Council, Hong Kong SAR; in part by a grant (SGDX20210823104003034) from the Science Technology and Innovation Committee of Shenzhen Municipality, China. (*Corresponding author:* C. Q. Jiang)

T. Ma, C. Jiang, X. Wang, J. Xiang, and L. Mo are with the Department of Electrical Engineering and the State Key Laboratory of Terahertz and Millimeter Waves, City University of Hong Kong, Hong Kong, China. Also, they are with City University of Hong Kong Shenzhen Research Institute, China (e-mail: tianlu.ma@my.cityu.edu.hk, chjiang@cityu.edu.hk, xiaoswang9-c@my.cityu.edu.hk, jinxiang2-c@my.cityu.edu.hk, lipingmo@ cityu.edu.hk).

K. T. Chau is with the Department of Electrical and Electronic Engineering, The Hong Kong Polytechnic University, Hong Kong, China (e-mail: k.t.chau@polyu.edu.hk).

and analyzed in detail to other non-isolated DC-DC converters. PEC has been applied to the WPT systems successfully [13] by measuring at most two voltages or currents for all compensated topologies where the energy calculation derivation is based on resonant networks, and it requires complex circuits to generate driving signals with variable frequency for the inverter. The idea of energy control is introduced to non-isolated DC-DC converters that account for more market share than WPT systems in this letter.

II. PEC Based on Buck Converters

The duty cycle is the control variable and is tuned by a control loop for most control methods. However, PEC is different from other control methods due to its distinctive control variable, the port energy. It aims to manage the energy going through one port. Assume the port voltage and current are u_p and i_p, and the switching period is T_s. The energy going through this port can be calculated by

$$E_p = \int_0^{T_s} u_p(t) i_p(t) dt \tag{1}$$

Therefore, the energy going through one port can be evaluated by testing port voltage and current. The active device can be switching devices, like MOSFET and IGBT. Meanwhile, non-isolated DC-DC converters are simple traditional topologies. The PEC applied to buck converters will be derived first in this section.

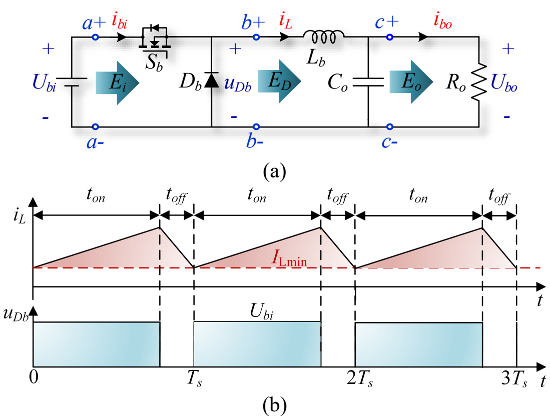

Fig. 1. The typical buck converter. (a) Equivalent circuit. (b) Main waveforms of the inductor current and diode voltage.

The topology of the buck converter is shown in Fig. 1(a). U_{bi}, U_{bo}, and u_{Db} are the voltages of input, output, and diode D_b. i_{bi}, i_{bo}, and i_L are the currents of input, output, and inductor L_b. The energy going through the input port (marked by nodes *a*+ and *a*-), output port (marked by nodes *c*+ and *c*-), and diode port (marked by nodes *b*+ and *b*-) are given by

$$\begin{cases} E_i = \int_0^{T_s} U_{bi}(t) i_{bi}(t) dt \\ E_o = \int_0^{T_s} U_{bo}(t) i_{bo}(t) dt \\ E_D = \int_0^{T_s} u_{Db}(t) i_L(t) dt \end{cases} \tag{2}$$

PEC is a control method that regulates the energy going through one port. The energy through these three ports can be regarded as a control target. Thus, the switches can be controlled such that the port energy meets the target energy during each switching period. The energy going through each of these three ports is equal if all components are lossless. However, in reality, $E_o < E_D < E_i$ due to the loss in the switches and passive components. The output voltage, current, or power are always target variables to be controlled. Therefore, E_o will be the best control target, considering the influence of the loss for PEC. However, the output voltage and current are both continuous even at the switching instant, and the control effect cannot be reflected in each switching period immediately if they are set to be control variables. Thus, E_o is not suitable for control strategies that require a fast response in each switching period, like PEC.

As a result, E_D is the optimal target for PEC, and the port voltage and current are shown in Fig. 1(b). T_s is the switching period, t_{on} and t_{off} are the time durations while S_b is on and off, respectively. It can be found that the inductor current is linear, and the voltage of D_b is constant during t_{on} or t_{off}.

The energy can be calculated by the integral of the port voltage and current over time, as shown in (2). However, once errors occur during the sampling and conversion process, they will be accumulated in the integral calculation. Thus, there might be a significant difference between calculated and actual results, which can make the system unstable for PEC. The conversion, in which the port energy is calculated by sampling several instantaneous voltages and currents instead of integral calculation, will be derived to increase the robustness of PEC and reduce the computational burden of the digital controller, which is very desirable for high-frequency operations.

As shown in Fig. 1(b), the port voltage u_{Db} is equal to the input voltage U_{bi} when S_b is on. And the input voltage equals 0 when S_b is off, which means there is no energy flowing into the load. Therefore, the energy E_D can be simplified as

$$\begin{aligned} E_D &= \int_0^{T_s} u_{Db}(t) i_L(t) dt \\ &= \int_0^{t_{on}} u_{Db}(t) i_L(t) dt \\ &= U_{bi} \int_0^{t_{on}} i_L(t) dt \end{aligned} \tag{3}$$

The state equation of the buck converter can be written when S_b is on, i.e.,

$$U_{bi} = L_b \frac{di_L}{dt} + U_{bo} \Rightarrow k_L = \frac{di_L}{dt} = \frac{U_{bi} - U_{bo}}{L_b} \tag{4}$$

where k_L is the slope of inductor current i_L when S_b is on, and the minimum value of inductor current $I_{L\min}$ occurs at the instant when S_b starts to turn on, namely, $t = nT_s$. Putting (4) in (3) gives

$$\begin{aligned} E_D &= U_{bi} \int_0^{t_{on}} i_L(t) dt = U_{bi} \int_0^{t_{on}} (k_L t + I_{L\min}) dt \\ &= U_{bi} \left(\frac{1}{2} k_L t^2 + I_{L\min} t + C \right) \Bigg|_0^{t_{on}} \\ &= U_{bi} \left(\frac{U_{bi} - U_{bo}}{2L_b} t_{on}^2 + I_{L\min} t_{on} \right) \end{aligned} \tag{5}$$

Therefore, E_D can be evaluated by the input voltage, output voltage, and minimum inductor current. U_{bi} and U_{bo} are

TABLE I. PEC APPLIED TO BASIC NON-ISOLATED DC-DC CONVERTERS

Topology	Equivalent circuit	Voltage gain	Simplified energy calculation	Conduction time
Buck converter	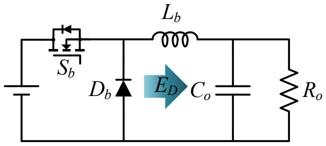	$\frac{U_o}{U_i}=D$	$E_D=U_i\left(\frac{1}{2}k_L t_{on}^2+I_{L\min}t_{on}\right)$ $k_L=\frac{U_i-U_o}{L_b}$	$t_{on}=\frac{-I_{L\min}+\sqrt{I_{L\min}^2+2k_L\frac{E_{tar}}{U_i}}}{k_L}$
Boost converter	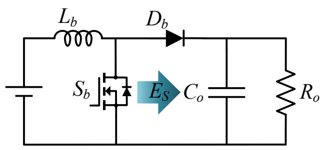	$\frac{U_o}{U_i}=\frac{1}{1-D}$	$E_S=U_o\left(-\frac{1}{2}k_L t_{off}^2+I_{L\min}t_{off}\right)$ $k_L=\frac{U_i-U_o}{L_b}$	$t_{off}=\frac{-I_{L\min}+\sqrt{I_{L\min}^2-2k_L\frac{E_{tar}}{U_o}}}{-k_L}$ $t_{on}=T_s-t_{off}$
Buck-boost converter	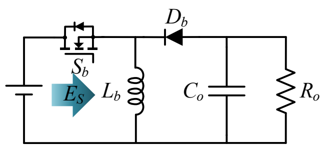	$\frac{U_o}{U_i}=\frac{-D}{1-D}$	$E_S=U_i\left(\frac{1}{2}k_L t_{on}^2+I_{L\min}t_{on}\right)$ $k_L=\frac{U_i}{L_b}$	$t_{on}=\frac{-I_{L\min}+\sqrt{I_{L\min}^2+2k_L\frac{E_{tar}}{U_i}}}{k_L}$
Zeta converter	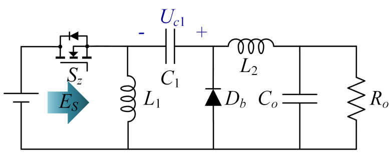	$\frac{U_o}{U_i}=\frac{D}{1-D}$	$E_s=U_i\left(\frac{1}{2}k_s t_{on}^2+I_{s\min}t_{on}\right)$ $k_s=\frac{U_i}{L_1}+\frac{U_i-U_o+U_{c1}}{L_2}$	$t_{on}=\frac{-I_{s\min}+\sqrt{I_{s\min}^2+2k_s\frac{E_{tar}}{U_i}}}{k_s}$

Note: U_i and U_o are the input and output voltages assumed to be constant in each switching period.

assumed to be constant in each switching period. Thus, these three variables can all be sampled at $t = nT_s$ to obtain U_{bi}, U_{bo}, and $I_{L\min}$.

For the implementation of PEC, the target energy E_{tar} will be given or tuned by another control loop. The conduction time of the switch t_{on} will be calculated to make E_D track E_{tar} in each switching period. The calculation of t_{on} for the buck converter can be derived by (5), i.e.,

$$t_{on}=\left(-I_{L\min}+\sqrt{I_{L\min}^2+2k_L\frac{E_{tar}}{U_{bi}}}\right)\bigg/k_L \tag{6}$$

III. PEC FOR OTHER NON-ISOLATED DC-DC CONVERTERS

The PEC based on the buck converter can be extended to other non-isolated DC-DC converters. The derivations are similar for other converters, and the results for four common non-isolated DC-DC converters are summarized in TABLE I. The features are as follows:

1) PEC will not affect the characteristics of the converters. The non-isolated DC-DC converter will be chosen according to the requirement of voltage gain.
2) The minimum inductor current $I_{L\min}$ or minimum current of the switch $I_{s\min}$ is needed for energy calculations, and it will be obtained by sampling the current at $t = nT_s$. In addition, the input and output voltages are also required for energy calculations in the buck, boost, and Zeta converters. However, the buck-boost converter does not need the output voltage to evaluate energy. Thus, the buck-boost converter can save hardware circuits and controller memories.
3) The buck, buck-boost, and Zeta converters share the same expression in energy calculation and conduction time. However, the slopes of the current (k_L or k_s) are different, which is determined by the topology.
4) The energy flows into the load when S_b is off for the boost converter. Therefore, the port energy is based on turn-off time t_{off}, and it can also be converted to turn-on time, $t_{on} = T_s - t_{off}$.

It should be noted that the calculation of the conduction time requires a square root operation, and a nonnegative real number is required. However, the solution of turn-off time for the boost converter may not meet this requirement all the time. For instance, the input voltage can be larger than the output voltage during the start-up process, in which a negative number may be presented for square root operation. Thus, the boost converter is not recommended for PEC.

To sum up, there are three basic principles that determine whether PEC can be applied to one non-isolated DC-DC converter. First, there should be at least one port of which the energy flowing depends on the switching action. Second, the port energy can be simplified (like the derivation of the buck converter in Section II). Third, simplified energy calculation must be suitable for all working conditions, and root operations on negative numbers are forbidden.

IV. VERIFICATION IN SIMULATIONS AND EXPERIMENTS

The simulations and experiments have been done to verify the proposed PEC. The buck converter is built by a half-bridge development board EPC9035, as shown in Fig. 3. The power inductor is manufactured by Würth Elektronik with a current rating of 11.2 A, and TI's TMS320F28377D generates PWM signals for driving the half-bridge. The input is connected to a DC power supply, and the output is connected to an electric load. Input and output filter capacitors are composed of six and four electrolytic capacitors of 220 μF, respectively. The system parameters are the same as TABLE II.

TABLE II. PARAMETERS OF THE BUCK CONVERTER

Symbol	Quantity	Value
L_b	Inductor	68 μH
C_o	Output filter capacitor	4*220 μF
C_{in}	Input filter capacitor	6*220 μF
R_o	Load resistance	10 Ω
U_{bi}	Input voltage	48 V
U_{bo}	Output voltage	36 V
f_s	Switching frequency	100 kHz

The simplified energy calculation and integral energy calculation methods are compared in simulations, as shown in Fig. 4. Numerical integration is used to simulate the implementation of the integral energy calculation in digital controllers. The simplified method has high accuracy both at transient and steady states.

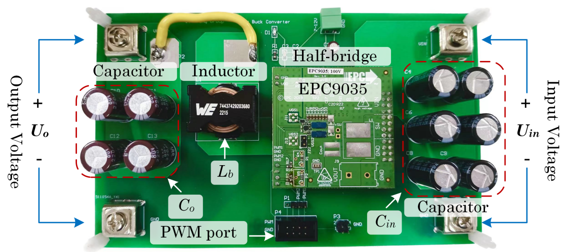

Fig. 3. Experiment setup of a synchronous buck converter using EPC9035.

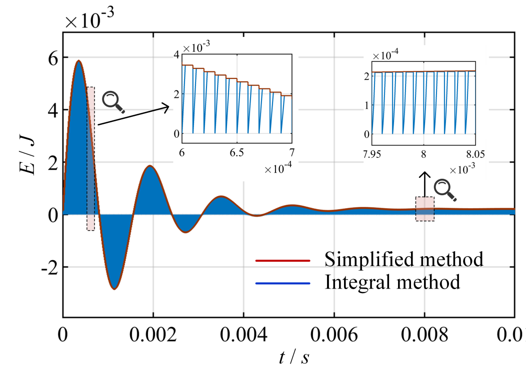

Fig. 4. Comparison of simplified and integral energy calculation, Duty cycle = 0.3, ESR of output filter capacitor is 0.1 Ω.

The experimental waveforms are shown in Fig. 2. The reference output voltage is 36 V, which is the commonly used battery voltage. The inductor current i_L, driving signal U_{dri}, input voltage U_{in}, and output voltage U_o are stable in steady-state operation, as shown in Fig. 2(a). The open-loop control is compared between the port energy step and duty cycle step, where the output voltage changes from 36 to 40 V, as shown in Fig. 2(b) and (c). The port energy or the duty cycle is changed by code in DSP directly. Although the adjustment time of the duty cycle step is quite shorter, the voltage overshoot and inductor current saturation both occur in the

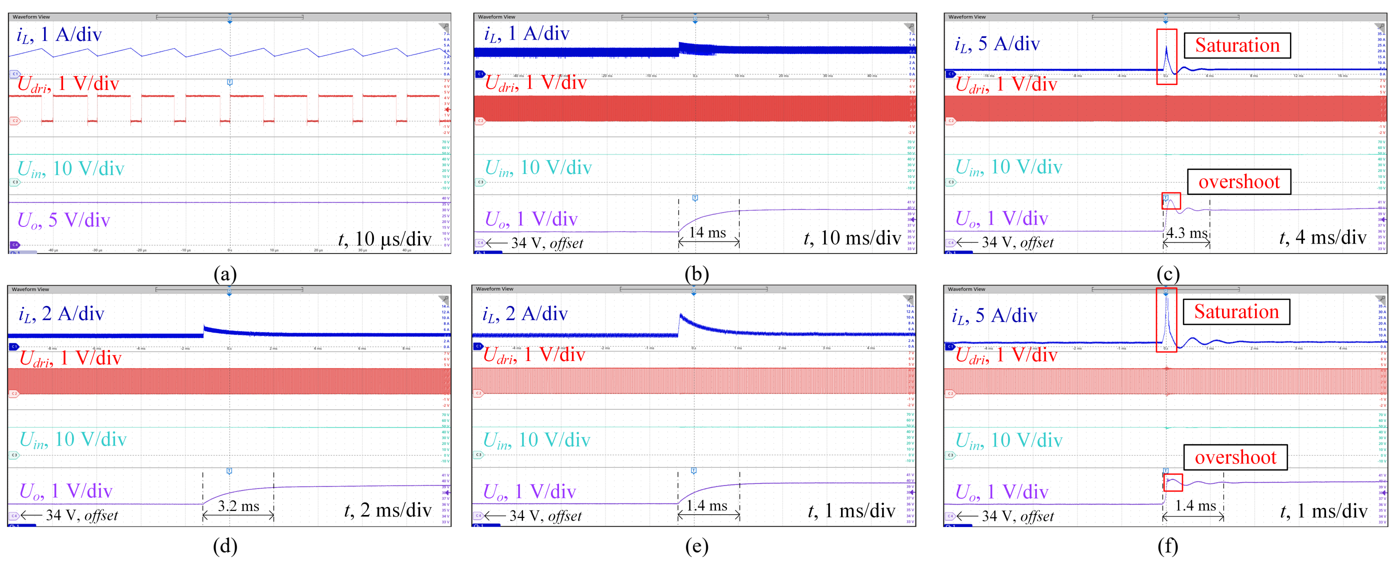

Fig. 2. Experimental waveforms of the buck converter. (a) Steady-state. (b) Port energy step while output voltage step from 36 to 40 V. (c) Duty cycle step while output voltage step from 36 to 40 V. (d) Single-loop PEC, K_p = 10, K_i = 400. (e) Single-loop PEC, K_p = 30, K_i = 400. (f) Single-loop PI control by tuning duty cycle, K_p = 150, K_i = 40000.

TABLE III. COMPARISON WITH PRIOR EXISTING WORKS.

Reference	Method	Control variable	Fixed switching frequency	Topology verified	Extended to other topologies	Computational complexity
[6]	Improved pulse width modulation	Duty cycle	Yes	Buck converter	No	Small
[7],[8]	Capacitor charge balance control	Charging and discharging time of capacitor	No	Buck converter	No	Small
[9]	Time optimal control	Charging and discharging time of capacitor	No	Buck converter	No	Small
[10]	Low frequency current-model control	Duty cycle	Yes	Boost converter	No	Medium
[12]	MPC	Three switching states	No	Buck-Boost converter	No	Large
This work	PEC	Port energy	Yes	Buck converter	Yes	Small

duty cycle step. The result showcases the advantage of PEC in overshoot suppression. In addition, closed-loop experiments with single-loop voltage control of PEC are conducted. The control diagram is shown in Fig. 5. Input voltage, output voltage, and inductor current are sensed with ratios of K_{ui} = 1/20, K_{iL} = 1/10, and K_{uo} = 1/20, which are used to calculate the conduction time by (6), and a PI controller is used to tune the target energy E_{tar} to regulate the system output voltage. Analog-to-digital converters, PI controller, conduction time calculation, and driving signals are all executed by DSP (blue zone in Fig. 5). The experimental waveforms are shown in Fig. 2(d) and (e) when the reference voltage steps from 36 to 40 V, which is conducted by programming code in DSP, and the adjustment time is reduced to 1.4 ms by increasing the proportional factor K_p from 10 to 30 with the same integral factor, K_i = 400. Similarly, a single-loop PI control by regulating the duty cycle instead of target energy is conducted, and the adjustment time is also 1.4 ms, whereas the output voltage overshoot and inductor current saturation exist both, as shown in Fig. 2(f). The numerous experimental results of single-loop PEC and traditional single-loop PI control by tuning duty cycle are summarized in Fig. 6, and the output voltage overshoot of PEC is smaller when the adjustment time is the same. Therefore, the proposed control method can suppress the overshoot effectively, which improves sustainability and reliability. The experimental results of load current stepping from 2 to 5 A under two kinds of single-loop controllers are also shown in Fig. 7, and the adjustment time is identical with low undershoot (both smaller than 200 mV), which illustrates the similar good performance during load current stepping.

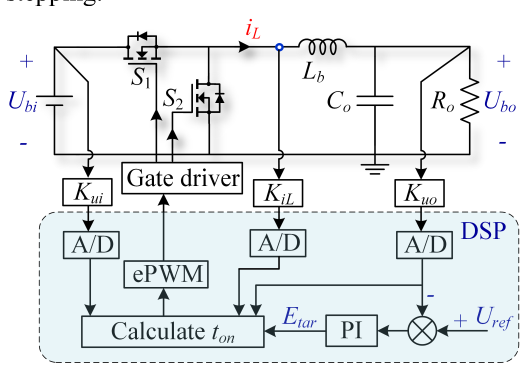

Fig. 5. The single-loop control diagram of PEC for the buck converter.

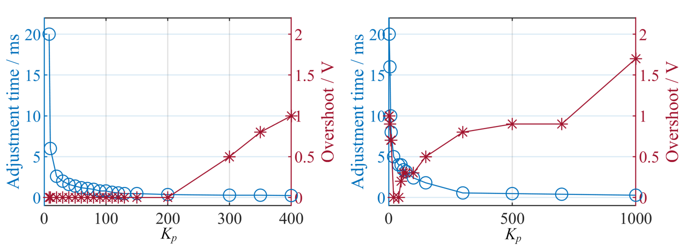

Fig. 6. The adjustment time and overshoot of the output voltage versus K_p when the reference voltage stepped from 36 to 40V. (a) Single-loop PEC, K_i = 400. (b) PI control by regulating the duty cycle, K_i = 40000.

A current limit can be used to avoid inductor current saturation in practical applications; however, it is not added in the experiment to illustrate the original features. By increasing the control loops, the performance of most of the control methods can be improved, including PEC, multiple simulations of dual-loop PEC and standard dual-loop PI control by tuning the duty cycle with different integral factors in the outer voltage loop are shown in Fig. 8, where the inductor current saturation is ignored and only the dual-loop control performance is studied. Dual-loop PEC has a lower peak in the inductor current than standard dual-loop PI control by tuning the duty cycle when they have the identical adjustment time within 1 ms, and there are similar conclusions for other proportional factors and integral factors in the inner current loop and outer voltage loop. In addition, the comparison with prior works is made in multiple aspects, as shown in TABLE III.

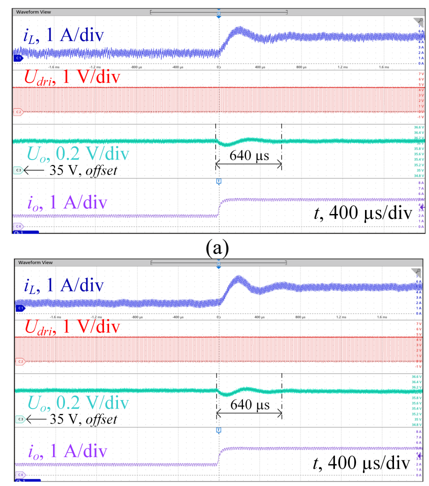

Fig. 7. The experiments of load current stepping from 2 to 5 A. (a) Single-loop PEC, K_p = 60, K_i = 2000000. (b) Single-loop PI control by tuning the duty cycle, K_p = 300, K_i = 500.

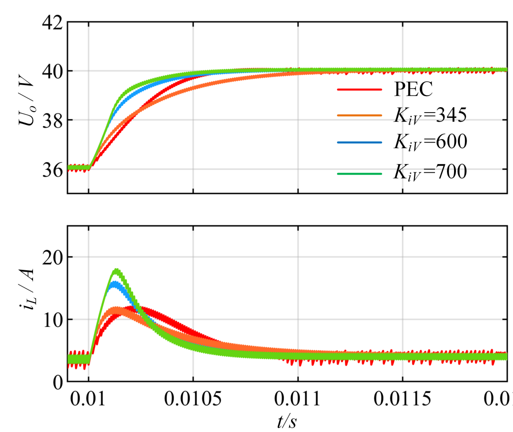

Fig. 8. Simulations of reference voltage stepping from 36 to 40 V for the dual-loop PEC (Inner loop: K_{pI} = 0.05, K_{iI} = 100; Outer loop: K_{pV} = 0.001, K_{iV} = 400) and standard dual-loop PI control by tuning the duty cycle with different integral factors in the outer voltage loop (Inner loop: K_{pI} = 1, K_{iI} = 800; Outer loop: K_{pV} = 0.01, K_{iV} = 345, 600, and 700).

V. CONCLUSIONS

A novel PEC for non-isolated DC-DC converters is proposed in this letter. The energy going through one port is the control target in PEC, which has a clear physical concept.

To reduce the computational burden of the digital controller, simplified energy calculation is derived and verified in simulations. Moreover, the proposed PEC has been extended to other typical non-isolated DC-DC converters. Open-loop, single-loop, and dual-loop control of PEC and duty cycle control are compared together in numerous experiments and simulations, and PEC can suppress the overshoot of the output voltage when the reference output voltage changes suddenly, allowing choosing a lower VA rating for capacitors or inductors. Therefore, it can improve the system's sustainability and reliability at a relatively low cost.

REFERENCES

[1] H. Li, J. Li, K. Wang, W. Chen, and X. Yang, "A Maximum Efficiency Point Tracking Control Scheme for Wireless Power Transfer Systems Using Magnetic Resonant Coupling," *IEEE Trans. Power Electron.,* vol. 30, no. 7, pp. 3998–4008, Jul. 2015.

[2] K. I. Hwu and Y. T. Yau, "Performance enhancement of boost converter based on PID controller plus linear-to-nonlinear translator," *IEEE Trans. Power Electron*., vol. 25, no. 5, pp. 1351–1361, May 2010.

[3] T. Kobaku, R. Jeyasenthil, S. Sahoo and T. Dragicevic, "Experimental verification of robust PID controller under feedforward framework for a nonminimum phase DC-DC boost converter," *IEEE Trans. Emerg. Sel. Topics Power Electron*., vol. 9, no. 3, pp. 3373-3383, Jun. 2021.

[4] E. Meyer, Z. Zhang, and Y. -F. Liu, "Controlled auxiliary circuit with measured response for reduction of output voltage overshoot in buck converters," in *Proc. IEEE Appl. Power Electron. Conf. Expo*., Feb. 2009, pp. 1367–1373.

[5] J. Wang et al., "A digitally controlled integrated DC-DC converter with transient suppression," in *Proc. 22nd Intern. Symp. Power Semiconductor Devices IC's (ISPSD)*, Jun. 2010, pp. 277–280.

[6] P. Kuo, Y. Lee, J. Lee, M. Huang, and H. Wang, "A low overshoot DC-DC buck converter with improved pulse width modulation technique," in *Proc. IEEE Conf. Consum. Electron. (ICCE-TW)*, Jul. 2022, pp. 385–386.

[7] E. Meyer, Z. Zhang, and Y. -F. Liu, "Digital charge balance controller to improve the loading/unloading transient response of buck converters," *IEEE Trans. Power Electron*., vol. 27, no. 3, pp. 1314–1326, Mar. 2012.

[8] L. Jia and Y. -F. Liu, "Low cost microcontroller based implementation of robust voltage based capacitor charge balance control algorithm," *IEEE Trans. Ind. Informat*., vol. 9, no. 2, pp. 869–879, May 2013.

[9] S. Kapat and P. T. Krein, "Improved time optimal control of a buck converter based on capacitor current," *IEEE Trans. Power Electron*., vol. 27, no. 3, pp. 1444–1454, Mar. 2012.

[10] P. Li, Y. Wang, L. Liu, X. Li, and Z. Zuo, "Low frequency current-mode control for DC-DC boost converters with overshoot suppression," *IEEE Trans. Circuits Syst. I, Reg. Papers*, vol. 69, no. 11, pp. 4702–4713, Nov. 2022.

[11] E. Garayalde, I. Aizpuru, U. Iraola, I. Sanz, C. Bernal, and E. Oyarbide, "Finite control set MPC vs. continuous control set MPC performance comparison for synchronous buck converter control in energy storage application," in *Proc. Int. Conf. Clean Electr. Power (ICCEP)*, Jul. 2019, pp. 490–495.

[12] B. Ullah and H. Ullah, "Finite control set model predictive control of noninverting buck-boost DC-DC converter," in *Proc. Int. Conf. Technol. Policy Energy Electr. Power (ICT-PEP)*, Oct. 2022, pp. 271–276.

[13] T. Ma, Y. Wang, X. Hu, D. Zhao, Y. Jiang, and C. Jiang, "Periodic energy control for wireless power transfer system," *IEEE Trans. Power Electron*., vol. 37, no. 4, pp. 3775–3780, Apr. 2022.